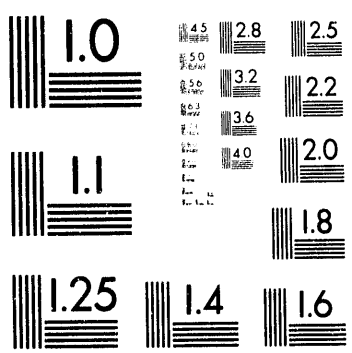
1.0
1.1
1.25
1.4
1.6
1.8
2.0
2.2
2.5
2.8
3.2
3.6
4.0
4.5
5.0
5.6
6.3

1 of 1

REDUCING INADVERTENT ALLOYING OF METAL/CERAMIC BRAZES

J. J. Stephens and P. F. Hlava

Materials and Process Sciences Center - 1800
Sandia National Laboratories
Albuquerque, NM 87185-5800

Abstract

Inadvertent alloying of Cu braze metal can compromise metal/ceramic seals by increasing the creep strength of the braze joint, thereby causing cracking in the ceramic. Electron microprobe analyses (EMPA) have quantified the alloying of Cu brazes in metal/ceramic feedthroughs. Pin material and processing parameters (peak temperature and time at temperature above 1084°C) both affect alloying levels. Using either Kovar™ (Fe-29Ni-17Co) or Ni-plated 316L stainless steel pins limits alloying as compared to using Palco™ (65wt.%Pd-35Co) pins. Minimizing the time during which the braze is molten also avoids excessive alloying. The original thickness of the Ni plating on the Mo-Mn metallization of the ceramic also influences the alloying content of these brazes.

Metal/ceramic brazes made with long brazing cycles, Mo-Mn metallization, and Kovar™ components grow a layer of intermetallic $Mo_6(Fe_{3.5}Co_{3.5})_7$ on the metallization. The presence of this layer suggests that the piece part was re-brazed using a belt furnace. The layer thicknesses observed do not appear to compromise joint integrity.

Previous work on creep strengthening of Cu by Class II solid solution alloying - in particular, the Cu-Ni system - permits a qualitative estimate of the creep properties of the alloyed brazements. Ni additions of approximately 10 and 20 wt. % to Cu apparently cause significant increases in the stress required to maintain creep rates required for stress relaxation during cooldown from the brazing temperature. Relative to unalloyed Cu, this strengthening effect tends to *increase* as temperature is decreased.

This work conducted at Sandia National Laboratories, supported by U.S. Dept. of Energy under contract number DE-AC04-76DP00789.

Note: "Kovar" is a registered trademark of Carpenter Technology Corporation, and "Palco" is a trademark of Wesgo, Inc.

Background

While process metallurgists recognize that extensive alloying of braze metal by base materials should be avoided (1), this is especially true for metal/ceramic brazes because they are designed to accommodate thermal expansion mismatches by stress relaxation of the braze metal and/or base metal (2). Factors influencing the final stress state in a metal/ceramic braze joint include the constituent materials and their mechanical properties, brazing parameters, and joint geometry. Shear-type braze joints, followed by tension-compression braze joints, offer the most potential for stress relaxation of the braze metal because they do not cause significant hydrostatic stresses (2).

This paper documents the results of an engineering and electron microprobe study aimed at reducing the level of alloying, and thereby controlling detrimental cracking of the ceramic, in a metal/ceramic "area seal" braze joint used for a vacuum-sealed, electronic component. Figure 1a is an optical micrograph of the specific area seal geometry under consideration. While all of the area seals discussed in this paper were made with braze preforms of electronic grade Cu (UNS #C10100), Kovar™ washers, and Mo-Mn metallized 94% alumina, the feedthrough pins were Kovar™, Ni-plated 316L stainless steel (316L SS), or Palco™. The seals are assembled in a fixture to permit belt-furnace brazing using a wet-hydrogen atmosphere.

Quantitative electron microprobe analyses reveal that pin material and parameters of the brazing cycle determine braze metal alloying levels. Long braze times with Palco™ pins cause extensive alloying of the braze metal which often lead to cracking in the ceramic as shown in Figures 1b and 1c (3,4). These cracks are quite frequent in rebrazed area seals with Palco™ pins, and less frequent in singly-brazed area seals using a 10 minute braze cycle with a peak temperature of 1109°C. These cracks also occur at a higher frequency following subsequent device processing - which includes an exhaust/pinch-off cycle of approximately 10 hrs. at 600°C.

Two types of cracks occur in the area seal geometry under consideration. Type A cracks (Figure 1b) extend from the end of the metallization into the bulk of the alumina ceramic at roughly a 30° angle while Type B cracks run along the interface between the alumina and the Mo-Mn metallization. While both types of cracks are undesirable, vacuum integrity for the ceramic part used in this assembly is not compromised until crack lengths exceed 200 μm. Thus Type B cracks, which are usually short compared to Type A cracks, tend to be less worrisome. Cracks are not always present; shorter braze cycle area seals have lower alloying levels in the braze metal and exhibit no significant cracking in the alumina.

Samples which were re-brazed using a 10 minute/1109°C brazing cycle formed a pseudo-binary Mo/Fe+Co intermetallic layer on the Mo-Mn metallization. While the presence of the intermetallic did not lead to problems with vacuum integrity, we include this information to fully document the microstructure of the metal/ceramic braze joint.

The correlation between alloying of the braze metal and cracking in the alumina is understandable in the context of solid solution strengthening of the Cu braze metal. Substitutional solid-solution alloying of Cu with Ni has a strong effect on decreasing the minimum creep rate. ~~And~~ Further as the alloying of the Cu

increases, creep-induced stress relaxation, during cooldown from the braze cycle, decreases, resulting in higher tensile stress in the braze and underlying ceramic. The buildup of tensile stress in the ceramic may be sufficient to crack it. Data from the literature on Cu-Ni alloys can be used to estimate the creep strength of the alloyed braze metals. The technique will be demonstrated in the final section of this paper.

Experimental Procedures

Brazing Conditions

All of the samples examined in this study have the geometry shown in Figure 1a. The 94% alumina was metallized with two coats of WESGO #547B metallization paint applied by brush with a firing at 1540°C for 35 minutes in a wet hydrogen atmosphere after each coat. The metallized surface was plated with a nominal thickness of 2.5 μm (100 microinches) of Ni then fired for 35 minutes at 960°C in wet hydrogen to eliminate residual gases. To insure that the desired geometry was obtained, all samples were brazed (with the pin end up) using 99% alumina fixtures. All of the area seals examined in this study were made with Cu (UNS #C10100) braze preforms and Kovar™ (Fe-29Ni-17Co) washers (see Figure 1a) and were brazed in a wet hydrogen atmosphere (dew point approximately 20-23°C). Belt furnace processing used hydrogen obtained from dissociated ammonia while batch furnace processing used bottled hydrogen gas.

A number of different brazing conditions were utilized to fabricate the samples examined. The majority of the samples were brazed in a three-zone BTU Transheat model #EGS-1 belt furnace using belt speeds that produced either a 3 or 10 minute thermal hold above the melting point of Cu (1084°C). Figure 3 of reference 2 shows the time-temperature record for a 10 minute thermal cycle with a peak temperature of 1109°C. The peak temperature indicated for a particular sample is based on the results of a calibration run using a dummy, thermocoupled assembly which recorded not only the peak temperature but also the entire thermal cycle of the braze.

Several Palco™ pin samples were made using a batch braze, Centorr Model 17 hydrogen furnace to demonstrate the minimum possible level of alloying in this assembly. The furnace was programmed to heat and cool the assemblies using a ramping profile which approximated that of the belt furnace. However, the time above 1084°C was the minimum necessary to achieve flow of the Cu braze metal. The cooldown cycle, also modeled after the braze cooldown cycle observed with the belt furnace, was -20°C/min. from 1084° to 1000°C; -70°C/min. from 1000° to 400°C; and -25°C/min. from 400°C to room temperature.

Metallographic Sample Preparation

All of the microprobed samples were prepared using techniques designed for optical metallography. Each sample was separately mounted in epoxy (Shell Epon 828 resin/DEA catalyst) and oriented to expose a longitudinal cross-section. The epoxy was mixed, then degassed under vacuum. After the samples were placed in molds and the epoxy added, they were placed under vacuum to assure complete impregnation. Flat "windows" prepared on the sides of the mounts and extreme care during grinding ensured ~~locating~~ that the diametrical

was located

(center) plane of each specimen. Samples were polished using 1 μm diamond paste, followed by 0.06 μm colloidal silica on a vibratory polisher. An electrically conductive layer of carbon was vacuum evaporated on each polished mount before microprobe analysis.

Electron Microprobe Techniques

The metallographically prepared samples were quantitatively examined with an automated JEOL (Japanese Electron Optics Laboratory) model 8600 electron microprobe x-ray analyzer controlled by use of the Sandia TASK8 software package (5). In addition, back-scattered and secondary electron images and elemental distribution photomicrographs of relevant areas were obtained to document trace paths. Pure metal standards were used to calibrate X-ray line positions and intensities for all the elements in these samples and for both operating modes. Most of the probe work utilized the instrument in the quantitative analysis mode (6) on long traces of hundreds of points approximately two microns apart. These analyses were performed using the instrument's wavelength dispersive detectors and an electronically stabilized beam of <1μm diameter at an accelerating voltage of 25 KeV and a current of approximately 25 nanoamperes. Quantitative analytical traces (or linescans, traverses, etc.) were defined by pairs of points and the analytical positions were spaced along those vectors at predetermined intervals. Two generic types of traces were acquired for these samples, as indicated in Figure 2: (a) the "Washer-to-Ceramic" (W-C) scans extended from the bottom end of the Kovar™ washer to the very end of the braze (b) the "Pin-to-Braze" (P-B) scans extended from the area seal pin into the braze parallel to the top of the Kovar™ washer. Average braze compositions were determined by selecting and averaging (7) data points which were positioned in the bulk of the braze metal: we excluded those analyses where the braze metal exhibited large gradients in alloying elements, such as at the edge of the braze adjacent to the pin. This paper emphasizes the results for the W-C scans because they reveal the composition of the braze immediately adjacent to the end of the braze fillet, where the highest stresses in the alumina ceramic are expected during cooldown from the brazing process (2).

Experimental Results and Discussion

Area Seals With Palco™ Pins: Effect of Brazing Time on Alloying of the Braze Metal

Palco™ pins and a long brazing cycle produce brazes that are highly alloyed. The brazing cycle is defined as the peak temperature and total "braze time," which is the time spent above the melting point of Cu (1084°C). Figure 3a is a plot (7) of the results from a W-C probe trace and it shows the composition of a highly alloyed braze. This sample was brazed in the belt furnace for 10 minutes at a peak temperature of 1109°C. The average composition of this braze, shown in Table 1, reveals a Cu content of only 89.57 wt. %: the Cu has dissolved over 10 wt. % of the other metals. The corresponding average composition for the "Pin-to- Braze" trace, shown in Table 2, reveals an average Cu content of 87.68 wt. %. A second, identical, braze cycle clearly increases the level of alloying in the braze as is shown in Figure 3b. When comparing Figures 3a and 3b, note that the Cu content in the single braze sample (Figure 3a) exceeds 90 wt. % at two sections of the scans but is always less than 90 wt. % in the re-brazed sample (Figure 3b).

Increasing the belt speed of the furnace lowers peak temperatures and significantly shortens braze times. This results in lower levels of alloying in area seals with Palco™ pins. Figure 4 is a compositional plot of the W-C trace of a sample brazed for 3 minutes with a peak temperature of 1097°C. Note that the average Cu content of this braze is higher than the longer cycle brazes. Similar results are shown in Table 1 for a 3 minute, 1100°C braze. These brazes have the minimum possible levels of alloying obtainable because faster belt speeds are not possible with the available belt furnaces.

Batch-type braze furnaces can produce Palco™ pin area seals whose brazes have lower levels of alloying than belt furnace brazes. The batch furnace results presented here represent the *minimum braze time* which can be achieved using this processing technique. Figure 5a shows the W-C probe results for an area seal brazed for 7 seconds above 1084°C with a peak temperature of 1087°C while Figure 5b shows the results for a second sample brazed for 6 seconds above 1084°C with a peak temperature of 1090°C. Average braze metal compositions for these samples, shown at the top of Tables 1 and 2, indicate that while alloying levels are quite low in both W-C traces, the P-B traces show significantly higher alloying. This is mainly due to the Pd in the braze metal and is undoubtedly caused by proximity to the Palco™ pin, source of the Pd, along with the high equilibrium solubility of Pd in Cu at the temperatures used.

Area Seals With Ni-Plated 316L Stainless Steel or Kovar™ Pins

Area seals brazed with Ni-plated 316L SS pins are more tolerant of long, belt-furnace braze cycles. This is illustrated in Figure 6 which shows the W-C probe results for an area seal containing a Ni-plated 316L SS pin brazed using a long (10 minute, 1109°C) belt-furnace cycle. The average composition of this braze (W-C trace shown in Table 1) is virtually identical to that of a sample with an identical pin brazed using the shorter (3 minute, 1097°C) belt-furnace braze cycle. Similar average compositions were also obtained from P-B results for these samples as shown in Table 2. These results suggest that the absence of Pd significantly reduces the alloying potential of the Cu braze metal.

Kovar™ pin results also indicate significantly lower alloying levels than for Palco™ pins, irrespective of braze cycle. Figure 7 shows the results of a W-C trace for a Kovar™ pin sample which was belt-furnace brazed for 3 minutes above 1084°C with a peak temperature of 1100°C. Average braze compositions for this sample are 94.74 wt. % Cu for the W-C trace (Table 1) and 94.84 wt. % Cu for the P-B trace (Table 2). Figure 8 also shows W-C results but for a sample brazed for 10 minutes above 1084°C with a peak temperature of 1106°C. This sample had a braze with average Cu contents of 94.95 wt. % (W-C) and 95.48 wt. % (P-B). Note that essentially all the probe data standard deviations for these Kovar™ pin samples overlap (see Tables 1 and 2). The one exception will be discussed in the next paragraph. The absence of Pd again correlates with less alloying. Even the alloying elements present (Ni, Fe and Co) are in lower concentrations suggesting that the presence of Pd in the Cu may increase the solubility of other metals in Cu.

Effect of Ni-Plate Thickness on Alloying of Braze Metal

The original thickness of the Ni-plate on the Mo-Mn metallized layer also affects alloying of the braze metal, to a minor degree, because it is completely dissolved into the Cu during brazing. W-C probe results for duplicate samples

processed under identical conditions (Table 1) show a significant variation in the amount of Ni measured. Note that while Fe, Co, and Pd contents for all three Palco pin samples brazed for 3 minutes vary slightly, the Ni content varies more. Kovar™ pin samples all show similar results (also Table 1). By contrast, the P-B probe results of the same samples show no significant variation in Ni content (Table 2), probably because of the distance from the P-B scan to the Ni-plated Mo-Mn metallization. The two Kovar™ pin samples brazed for 10 minutes with a peak temperature of 1106°C are especially illustrative. The average Ni content of the braze in the W-C area was 2.97 wt. % in one sample and 4.20 wt. % in the second sample. Extra care was taken to insure that the two microprobe traces traversed the braze along identical paths, i.e. at an equal angle or starting and ending distances from the Mo-Mn metallization. SEM photos, taken after the quantitative analyses, clearly show the identical positions of the probe contamination marks. These data force us to attribute compositional differences in these samples to differences in the thickness of the Ni plate (now completely dissolved into the braze) on the Mo-Mn metallization. Unfortunately we cannot quantify sample-to-sample variations in Ni plate thicknesses because we did not examine "as-plated" ceramic bodies prior to brazing. However, we have noticed that some samples have unusually large amounts of Ni-plate near the end of the metallization, past the position where the braze thins out. It is not unreasonable to expect significant variations in the Ni-plate thickness. Controlling Ni plate thickness should help to minimize alloying of the Cu in the most critical region of these brazes .

Solubility of the Various Elements in Cu

Table 3 lists data on the equilibrium solubility in Cu for the elements and brazing temperatures of interest (1100 and 1110°C). These numbers are based on *binary* equilibrium systems: unfortunately, phase diagrams of the appropriate ternary systems are not available. Table 3 shows that the equilibrium solubility for Pd (either weight % or atomic %) in Cu is substantially higher than that of Ni, Fe, or Co. Pd also appears to increase the total amount of alloying possible in a Cu braze. It is therefore important to avoid process cycles that create equilibrium, or near-equilibrium, conditions when using Cu to braze Pd-containing alloys such as Palco. This, in turn, implies that batch-furnace brazing is better than belt-furnace brazing for processing Pd-bearing alloys because the batch method can easily reduce the time that the braze is molten by more than an order of magnitude.

Formation of a Mo-Fe-Co Intermetallic Compound in Re-brazed Samples

A layer containing primarily Mo, Co, and Fe forms on the Mo-Mn metallization in long-cycle, rebrazed, Palco™ pin samples. This layer appears to form when Co and Fe, dissolved into the Cu braze and diffused away from the Kovar™ washer, react with the Mo-Mn metallization exposed by the dissolution of the Ni-plate. Total length of braze time (20 minutes), rather than re-flowing, appears to be responsible for continuous layers of this material. Secondary electron (Figure 9a) and back-scattered electron images (Figure 9b) of a re-brazed sample show this reaction layer. The layer is marked by arrows and, in Figure 9b, is intermediate in gray tone between the darker Cu braze metal and the lighter Mo metallization. Quantitative analyses (Table 4) indicate that the material is close in composition to the pseudobinary $Mo_6(Fe_{3.5}Co_{3.5})_7$ with

minor level of Ni and Cu present (the actual, complete formula is $Mo_6(Co_{3.21}Fe_{2.75}Ni_{.62}Cu_{.42})_7$). That is, the material appears to be the binary Mo_6Co_7 with nearly half the Co replaced by Fe, etc. The average Mo content of 46.13 at. % confirms the Mo_6Co_7-like compound. The Mo-Fe phase diagram also exhibits an intermetallic compound (Mo_6Fe_7) with the same stoichiometry and crystal structure as Mo_6Co_7.

The presence of this reaction layer in and of itself does not appear to compromise the vacuum integrity of the area seal but it does serve as evidence of excessive brazing time. Etter, et. al. (8) observed (qualitatively) a Mo-Fe-Co-Ni compound on the Mo-Mn metallization in an alumina seal Ag-brazed to Kovar™. They observed that Fe, Co, and Ni had dissolved from the Kovar™, migrated across the Ag braze, and reacted with the Mo-Mn metallization. The low solubility of Ni in Ag explains why Ni is found in their intermetallic but not in the Ag braze metal. The high solubility of Ni in Cu explains why Ni is found in the Cu braze metal but is not a major element the intermetallic reported in this paper. Long Ag-braze times were again responsible for the observed reaction layer (8).

Effect of Solid Solution Alloying on the Creep Properties of Cu

All of the experimental results obtained in this study indicate that solid-solution alloys are formed in the braze as a result of Cu (UNS #C10100) preforms alloying with dissolved (a) pin material, (b) Kovar™ washer material, and (c) the Ni plate on the Mo-Mn metallization. While the actual, measured, compositions are multicomponent in nature, it is nevertheless instructive to consider the effect on creep properties of binary, Cu-based, Class II solid-solution alloys which have been examined in the literature (9). The Cu-Ni system is an obvious choice because it has been extensively studied and closely models the present system. We will briefly examine data from two previous investigations: the study of Jones and Sellars (10), that examined the creep properties of a Cu-9.18 wt. % Ni alloy (Cu-9.86 at. % Ni) at 600° and 800°C and the study of Monma, et. al. (11), that examined a number of compositions across this system at homologous temperatures in excess of ~0.58. In the following paragraphs we examine steady-state, creep-rate data from these investigations and compare them to the creep correlation developed for pure Cu in reference 2.

Monma, et. al. (11) characterized the steady-state creep-rate (ε_{ss}) of Cu-20.2 wt. % Ni (Cu-21.5 at. % Ni) alloy at temperatures ranging from 541° to 1006°C, and at stresses ranging from 13.7 MPa to 42.2 MPa, with the following power law equation:

$$\varepsilon_{ss}\ (s^{-1}) = 2.428\ (\sigma(MPa))^{4.80} \exp(-56{,}500\ (cal/mole)/RT) \qquad (1)$$

where σ is the true stress in MPa, R is the gas constant (1.987 cal/mole/Kelvin) and T is the absolute temperature in Kelvin. Multivariable linear-regression analysis of the 600° and 800°C data of Jones and Sellars (10) for the Cu-9.18 wt. % Ni alloy leads to a power law equation as follows:

$$\varepsilon_{ss}\ (s^{-1}) = 6.221\ (\sigma(MPa))^{4.95} \exp(-56{,}021\ (cal/mole)/RT) \qquad (2)$$

with a correlation coefficient (r^2) of 0.992. Note that the activation energy for creep obtained from this data is very close to that of Monma, et. al. (11) for the Cu-20.2 wt. % Ni alloy.

Figure 10 is a comparison of the steady-state creep properties of Cu-9.18 wt. % Ni, Cu-20.2 wt. % Ni, and the correlation for pure Cu developed in ref. 2 at 800° and 600°C. Figure 10a indicates that both Cu-9.18 wt. % Ni and Cu-20.2 wt. % Ni are significantly stronger than Cu at 800°C. This is normal for a Class II solid-solution alloy. These alloys are even stronger, relative to pure Cu, at 600°C (Figure 10b and Table 5). This divergence in strength as a function of temperature is caused by the decreasing activation energy for creep of pure Cu (from 53.8 kcal/mole at 800°C to 35.8 kcal/mole at 600°C). Other data (12) suggest that the activation energy for creep of Cu-Ni alloys should decrease to a similar value (37.2 kcal/mole for a Cu-13.63 wt. % Ni alloy) at ~500°C rather than 600°C. Thus the net effect of the Ni additions is to extend the high temperature creep characteristics (high activation energy) to lower temperatures, thus strengthening the alloy. Similar effects should occur in alloys containing the other metals of interest here.

A useful indicator of the amount of stress-relaxation possible in the braze alloy is the stress required to produce a steady-state creep-rate of 10^{-7} s^{-1} at a given temperature during cooldown (since 10^{-7} s^{-1} would be a typical strain rate *if* stress relaxation occurs). The cooldown rate of the braze cycle has a very strong influence on the creep rate. Table 5 data indicate that alloying levels of 9 wt. % Ni substantially strengthen the braze leading to increased tensile stresses in the ceramic, especially at the high stress region close to the end of the braze fillet (13). This is consistent with the observation that significant cracking in the ceramic is observed only when there is a substantial amount of alloying in the braze metal.

Summary and Conclusions

1. Belt-furnace processed metal/ceramic area seals with a Cu braze metal that have either a Kovar™ or Ni-plated 316L SS pin were found to exhibit significantly less alloying than those brazed with Palco pins. The alloying level of Cu to Palco pin brazes can be minimized by utilizing a batch brazing furnace that significantly reduceds the length of time that the braze alloy is molten during brazing.

2. Sample-to-sample variations in Ni-plate thickness on the Mo-Mn metallization layer appear have a measurable effect on the amount of alloying observed in the "Washer-to-Ceramic" traces for experimental conditions where multiple samples were examined.

3. Long braze times with a Kovar™ washer close to Mo-Mn metallization have been shown to form a ternary Mo-Fe-Co reaction layer. This reaction layer has been found to also include Ni and Cu in small amounts, but appears to be close in composition to the compound $Mo_6(Fe_{3.5}Co_{3.5})_7$.

4. A survey on the effect of Class II solid solution alloying additions to Cu on creep properties has indicated that Cu-Ni have been extensively studied. The results for Cu-Ni suggest that, at intermediate temperatures of 600° and 800°C, a 10 wt. % Ni addition to Cu serves to roughly double the stress required to

maintain a steady state strain rate of 10^{-5} to 10^{-7} s^{-1} compared to pure Cu. These results suggest that minimal alloying is most desirable for Cu brazes when metal-ceramic brazes are being considered.

Acknowledgments

We would like to acknowledge the contributions of L. C. Beavis, SNL Dept. 2471, for his help in designing the batch, braze furnace experiments and of A. C. Kilgo, SNL Dept. 1822 for her metallographic preparation of the samples. The contributions of F. M. Hosking, SNL Dept. 1831, during review of this paper are also appreciated. Finally, we would like to acknowledge the project support for this study, provided by J. A. Wilder, SNL Dept. 2574, and E. M. Austin, SNL Dept. 336.

References

1. AWS Committee on Brazing and Soldering, Brazing Handbook, 4th Edition, Miami, Florida: American Welding Society, 1991, p. 43.

2. J. J. Stephens, S. N. Burchett and F. M. Hosking, "Residual Stresses in Metal/Ceramic Brazes: Effect of Creep on Finite Element Analysis Results", in P. Kumar and V. A. Greenhut (eds.), Metal-Ceramic Joining, Warrendale, PA: TMS, 1991, pp. 23-41.

3. A. Shuman and L. Beavis (eds.), "Proceedings of the First Switch Tube Advanced Technology Meeting", SAND90-2172, Sandia National Laboratories, May, 1991, pp. 61-64, 116-118.

4. J. J. Stephens, et. al., Internal Memorandum to J. A. Wilder, Sandia National Laboratories, New Mexico, 8 November 1990.

5. W. F. Chambers and J. H. Doyle, "SANDIA TASK8, Version C: A Subroutined Electron Microprobe Automation System", SAND90-1703, Sandia National Laboratories, December, 1990.

6. W. F. Chambers and J. H. Doyle, "Quantitative Analysis Procedures for TASK 8", SAND90-1704, Sandia National Laboratories, January, 1991.

7. W. F. Chambers and J. H. Doyle, "Plotting and Summary Routines for TASK8", SAND90-1701, Sandia National Laboratories, December, 1990.

8. D. E. Etter, E. E. Egleston, and R. R. Jaeger, "The Migration of Iron, Nickel, Cobalt, and Chromium Associated with Silver Brazing During Ceramic-To-Metal Joining," Miamisburg, Ohio: Mound Facility, Report MLM-2526, June 30, 1978.

9. O. D. Sherby and P. M. Burke, "Mechanical Behavior of Crystalline Solids at Elevated Temperature," Progress in Materials Science, 13 (1968), 324-390.

10. B. L. Jones and C. M. Sellars, "The Creep of Copper, Copper-10 at. % Nickel and Copper-10 at. % Gold Alloys," Metal Science Journal, 4 (1970), 96-102.

11. K. Monma, H. Suto and M. Oikawa, "High Temperature Creep of Nickel-Copper Alloys," Journal of Japanese Institute of Metals, 28 (1964), 253-258.

12. I. D. Choi, D. K. Matlock and D. L. Olson, "Creep Behavior of Nickel-Copper Solid Solution Alloys Below 0.55 Tm," Metallurgical Transactions, 21A (1990), 2601-2605.

13. E. K. Beauchamp and S. N. Burchett, "Techniques of Seal Design," in S. J. Schneider, Jr. (ed.), Engineered Materials Handbook, Volume 4: Ceramics and Glasses, Materials Park, Ohio: ASM International, 1991. p. 538.

Figure Captions

Figure 1 Metallographic cross sections (diametral plane) of the "area seal" geometry discussed in this paper. (a) Overall view, with identification of the construction materials. This particular area seal has a Palco™ pin and was brazed in a belt furnace for a total of 3 minutes above 1084°C, with a peak temperature of 1097°C. Both (b) and (c) are from different samples and show a layer of Ni plated onto the Cu braze metal - the Cu/Ni interface is marked by the upper set of arrows. (b) Type A crack (lower arrows) proceeding into the bulk of the alumina ceramic. (c) Type B crack (lower arrows) running along the interface between the Mo-Mn metallization and the alumina ceramic.

Figure 2 Schematic diagram showing the locations of the "Washer to Ceramic" and "Pin to Braze" electron microprobe traces on the brazed, area-seal samples.

Figure 3 Plots of electron microprobe results for "Washer-to-Ceramic" traces on two Palco™ pin, area-seal samples brazed using a belt-furnace and long braze cycles (10 minutes above 1084°C with a peak temperature of 1109°C). (a) Singly-brazed sample with an average Cu content, in this section of the braze, equal to 89.57 wt. %. (b) Re-brazed sample with an average Cu content, in the same section of this braze, equal to 86.96 wt. %.

Figure 4 Plots of electron microprobe results for "Washer-to-Ceramic" traces on a Palco™ pin, area-seal sample brazed using a belt-furnace and short braze cycle (3 minutes above 1084°C with a peak temperature of 1097°C). The average Cu content in this section of the braze is equal to 92.76 wt. %.

Figure 5 Plots of electron microprobe results for "Washer-to-Ceramic" traces on a Palco™ pin, area-seal sample brazed using a batch furnace and the shortest possible braze cycle. (a) Area seal brazed using a thermal cycle of 7 seconds above 1084°C and a peak temperature of 1087°C. The average Cu content in this section of the braze is 99.68 wt. %. (b) Area seal brazed using a thermal cycle of 6 seconds above 1084°C with a peak temperature of 1090°C. The average Cu content in this section of the braze metal is 98.75 wt. %.

Figure 6 Plots of electron microprobe results for "Washer-to-Ceramic" traces on a Ni-plated 316L stainless steel pin, area-seal sample brazed using a belt-furnace and a braze cycle of 10 minutes above 1084°C with a peak temperature of 1109°C.

Figure 7 Plots of electron microprobe results for "Washer-to-Ceramic" traces on a Kovar™ pin, area-seal sample brazed using a belt-furnace and a braze cycle of 3 minutes above 1084°C with a peak temperature of 1100°C.

Figure 8 Plots of electron microprobe results for "Washer-to-Ceramic" traces on a Kovar™ pin, area-seal sample brazed using a belt-furnace and a braze cycle of 10 minutes above 1084°C with a peak temperature of 1106°C. The average Cu content in this section of the braze is 94.95 wt. %

Figure 9 Scanning electron micrographs of the interfacial region showing the braze metal, Mo-Mn metallization and the alumina ceramic in a sample which was apparently re-brazed using the ten minute/1109°C cycle described in Figure 3. In both photos, the region between the arrows consists of the pseudobinary Mo-Fe-Co intermetallic compound roughly corresponding to $Mo_6(Fe_{3.5}Co_{3.5})_7$. (a) Secondary electron image. (b) Back-scattered electron image.

Figure 10 Graph illustrating the effect of increasing Ni content on the steady-state creep rate of Cu alloys. Data on Cu-20.2 wt. % Ni are from Monma, et. al. (11), while the data for Cu-9.82 wt. % Ni are from Jones and Sellars (10). The correlations for pure Cu were developed in ref. 2. (a) Effect of alloying with Ni on the creep properties at 800°C. (b) Effect of alloying with Ni on the creep properties at 600°C.

Table 1. Average "lower braze" compositions: the results of "Washer-to-Ceramic" traces depicted in Figure 2. Normalized electron microprobe results in wt. % with standard deviations shown in parenthesis. Unless otherwise indicated as "batch" processed, the brazing was done using a belt furnace; all brazing was done in a wet hydrogen atmosphere. Times shown denote the time spent above the melting point of Cu (1084°C) and the temperatures shown indicate the peak temperature achieved during the run. "2x" denotes that a sample was subjected to a second brazing operation.

Braze Conditions	Fe	Co	Ni	Cu	Pd
Brazes w/Palco™ Pin					
Batch/6 sec./1090°C	0.27(0.08)	0.10(0.04)	0.82(0.32)	98.75(0.56)	0.06(0.02)
Batch/7 sec./1087°C	0.11(0.06)	0.01(0.02)	0.20(0.13)	99.68(0.49)	0.01(0.01)
3 min./1097°C	1.41(0.51)	0.66(0.20)	4.08(2.18)	92.76(2.70)	1.09(0.10)
3 min./1097°C	1.28(0.21)	0.66(0.12)	3.21(0.65)	93.44(0.95)	1.42(0.05)
3 min./1100°C *	1.29(0.33)	0.59(0.18)	2.51(0.62)	94.22(1.10)	1.32(0.09)
10 min./1109°C	1.96(0.45)	1.16(0.26)	4.75(0.89)	89.57(1.48)	2.55(0.13)
2x 10 min./1109°C **	2.39(0.76)	1.62(0.60)	3.47(0.94)	86.96(2.22)	5.44(0.09)
Brazes w/Ni Plated 316L Pin					
3 min./1097°C ***	1.35(0.32)	0.40(0.12)	3.72(0.93)	94.52(1.39)	----------
10 min./1109°C ****	1.61(0.19)	0.30(0.06)	3.91(0.42)	94.14(0.53)	----------
Brazes w/Kovar™ Pin					
3 min./1100°C +	1.65(0.53)	0.26(0.18)	2.72(1.19)	95.32(1.50)	----------
3 min./1100°C ++	1.62(0.33)	0.49(0.11)	3.12(0.88)	94.74(1.34)	----------
10 min./1106°C +++	1.94(0.29)	0.53(0.09)	4.20(0.69)	93.28(1.14)	----------
10 min./1106°C ++++	1.57(0.20)	0.43(0.06)	2.97(0.43)	94.95(0.62)	----------

* 0.04(0.05) Mo and 0.02(0.04) Au were also measured.
** 0.02(0.03) Si, 0.03(0.01) Cr, 0.04(0.01) Mn, and 0.03 (0.02) Mo were also measured.
*** 0.01(0.01) Mn was also measured.
**** 0.01(0.01) Mn and 0.02(0.01) Mo were also measured.
\+ 0.02(0.01) Mn and 0.03(0.02) Mo were also measured.
++ 0.01(0.01) Mn, 0.01(0.00) Cr and 0.01(0.01) Mo were also measured.
+++ 0.02(0.04) Al, 0.02(0.01) Mn and 0.02(0.02) Mo were also measured.
++++ 0.04(0.07) Al, 0.02(0.01) Mn and 0.02(0.03) Mo were also measured.

Table 2. Average "upper braze" compositions: results of "Pin-to-Braze" traces depicted in Figure 2. Normalized electron microprobe results in wt. %, standard deviations are shown in parenthesis. Same remarks apply as in Table 1.

Braze Conditions	Fe	Co	Ni	Cu	Pd
Brazes w/Palco™ Pin					
Batch/6 sec./1090°C	0.44(0.13)	0.59(0.13)	0.18(0.08)	97.42(0.51)	1.38(0.10)
Batch/7 sec./1087°C	0.17(0.06)	0.31(0.06)	0.05(0.03)	98.48(0.40)	0.99(0.13)
3 min./1097°C	1.60(0.44)	1.82(0.49)	1.68(0.39)	91.11(1.38)	3.79(0.14)
3 min./1097°C	1.55(0.44)	1.76(0.52)	1.87(0.46)	91.18(1.62)	3.65(0.06)
10 min./1109°C	2.09(0.76)	2.27(1.01)	3.04(0.76)	87.68(2.58)	4.92(0.23)
2x 10 min./1109°C	1.78(0.49)	1.95(0.61)	2.72(0.67)	87.55(1.92)	6.01(0.20)
Brazes w/Ni Plated 316L Pin					
3 min./1097°C	1.58(0.37)	0.52(0.14)	3.56(0.83)	94.32(1.26)	----------
10 min./1109°C	1.47(0.27)	0.29(0.12)	3.86(1.03)	94.38(1.39)	----------
Brazes w/Kovar™ Pin					
3 min./1100°C *	2.01(0.43)	0.42(0.16)	2.67(0.63)	94.84(1.10)	----------
10 min./1106°C **	1.71(0.36)	0.48(0.13)	2.41(0.55)	95.32(1.07)	----------
10 min./1106°C ***	1.59(0.43)	0.43(0.15)	2.42(0.68)	95.48(1.32)	----------

* 0.03(0.00) Mn, 0.01(0.00) Cr and 0.02(0.02) Mo were also measured.
** 0.03(0.10) Al, 0.03(0.01) Mn and 0.01(0.02) Mo were also measured.
*** 0.04(0.07) Al, 0.02(0.01) Mn and 0.01(0.02) Mo were also measured.

Table 3. Equilibrium solubility of Co, Fe, Ni and Pd, respectively, in molten Cu at 1100°C and 1110°C. Data shown are for binary systems. (Data from T. R. Massalski, Binary Alloy Phase Diagrams, ASM, 1986)

Solute Element	Equilibrium Solubility, wt. % (at. %) in Molten Cu at:	
	1100°C	1110°C
Cobalt	2.79(3.00)	4.63(4.97)
Iron	3.63(4.11)	3.87(4.38)
Nickel	2.94(3.18)	3.85(4.15)
Palladium	15.87(10.13)	21.11(13.78)

Table 4. Results of quantitative point analyses in wt. % (with normalized atomic % shown in parenthesis) of the intermetallic layer (primarily Mo-Fe-Co) found in a sample which had been rebrazed, i.e., processed through two belt furnace cycles consisting of 10 minutes above 1084°C with a peak temperature of 1109°C. Analyses were performed using K_α lines for all elements except Mo, where the L_α line was used. "Pure compound" refers to the calculated composition for stoichiometric $Mo_6(Fe_{3.5}Co_{3.5})_7$.

Point #	Fe	Co	Ni	Cu	Mo
1	15.31(20.72)	19.29(24.74)	3.48(4.48)	2.46(2.92)	59.84(47.14)
2	15.50(20.98)	18.76(24.07)	3.90(5.02)	4.23(5.04)	56.96(44.89)
3	15.62(21.29)	19.06(24.62)	3.77(4.89)	2.05(2.46)	58.90(46.73)
4	15.38(20.85)	19.84(25.50)	3.61(4.65)	2.04(2.43)	59.00(46.57)
5	16.37(22.10)	19.27(24.67)	3.68(4.73)	2.69(3.20)	57.63(45.30)
Avg.	15.64(21.19)	19.24(24.72)	3.69(4.75)	2.69(3.21)	58.47(46.13)
Pure Compound	*20.00(26.92)*	*21.10(26.92)*	--------	-------	*58.90(46.15)*

Table 5. Stress, σ(MPa), necessary to generate steady-state creep rates of 10^{-5} and 10^{-7} s^{-1} at 600° and 800°C, respectively, for Cu, Cu-9.18 wt. % Ni (Cu-9.86 at. % Ni) and Cu-20.2 wt. % Ni (Cu-21.5 at. % Ni). Data for the alloys were obtained for references 10 and 11, and the correlation for Cu is from reference 2.

SS. Creep Rate, s^{-1}	σ (MPa) Necessary to Obtain Desired Steady-State Creep Rate for:		
	Cu	Cu-9.18 Ni	Cu-20.2 Ni
At 800°C:			
10^{-5}	7.96	13.67	18.98
10^{-7}	2.56	5.38	7.25
At 600°C:			
10^{-5}	24.49	46.01	66.99
10^{-7}	6.59	18.11	25.62

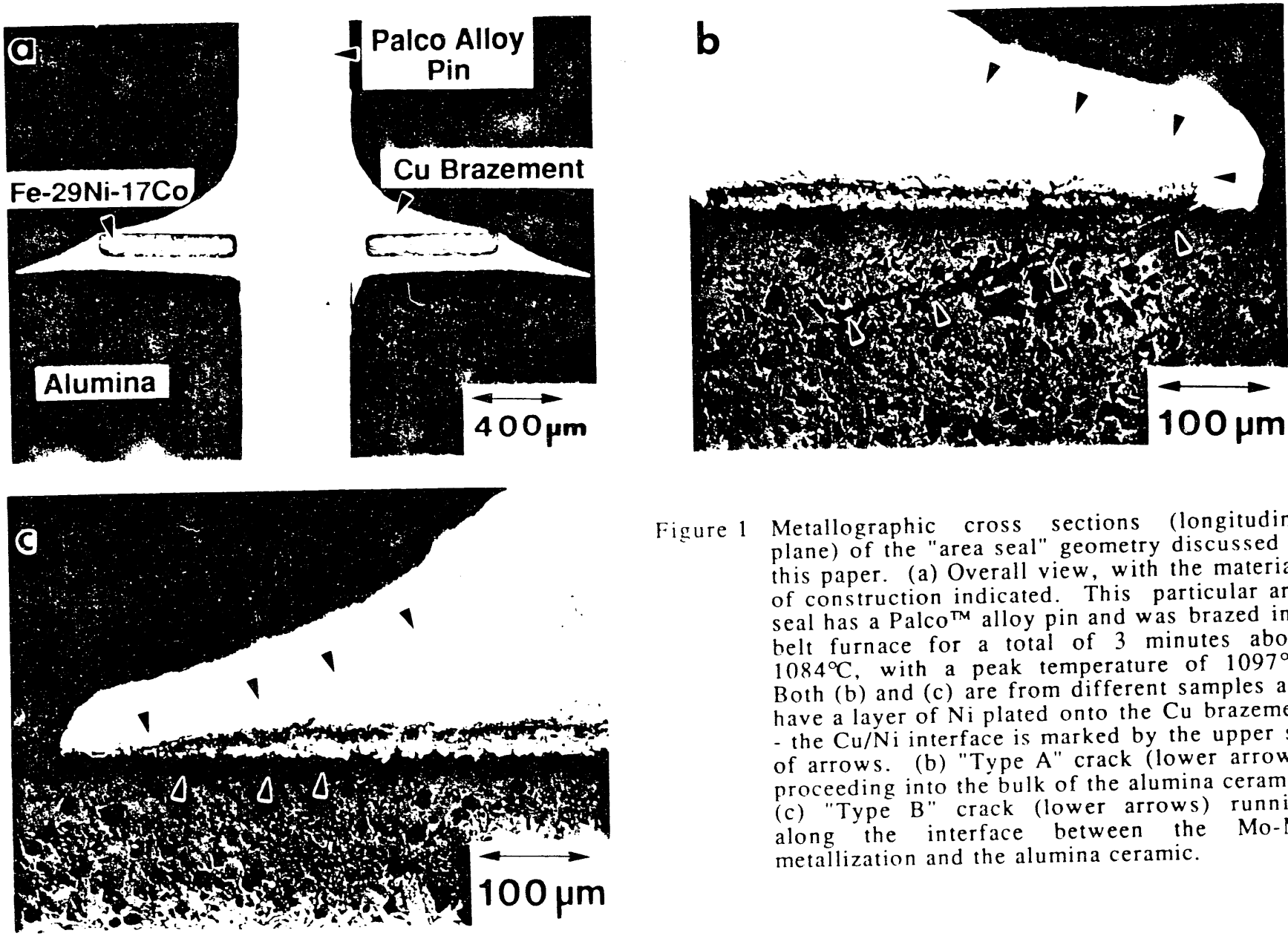

Figure 1 Metallographic cross sections (longitudinal plane) of the "area seal" geometry discussed in this paper. (a) Overall view, with the materials of construction indicated. This particular area seal has a Palco™ alloy pin and was brazed in a belt furnace for a total of 3 minutes above 1084°C, with a peak temperature of 1097°C. Both (b) and (c) are from different samples and have a layer of Ni plated onto the Cu brazement - the Cu/Ni interface is marked by the upper set of arrows. (b) "Type A" crack (lower arrows) proceeding into the bulk of the alumina ceramic. (c) "Type B" crack (lower arrows) running along the interface between the Mo-Mn metallization and the alumina ceramic.

ELEMENTAL PROBE TRACES

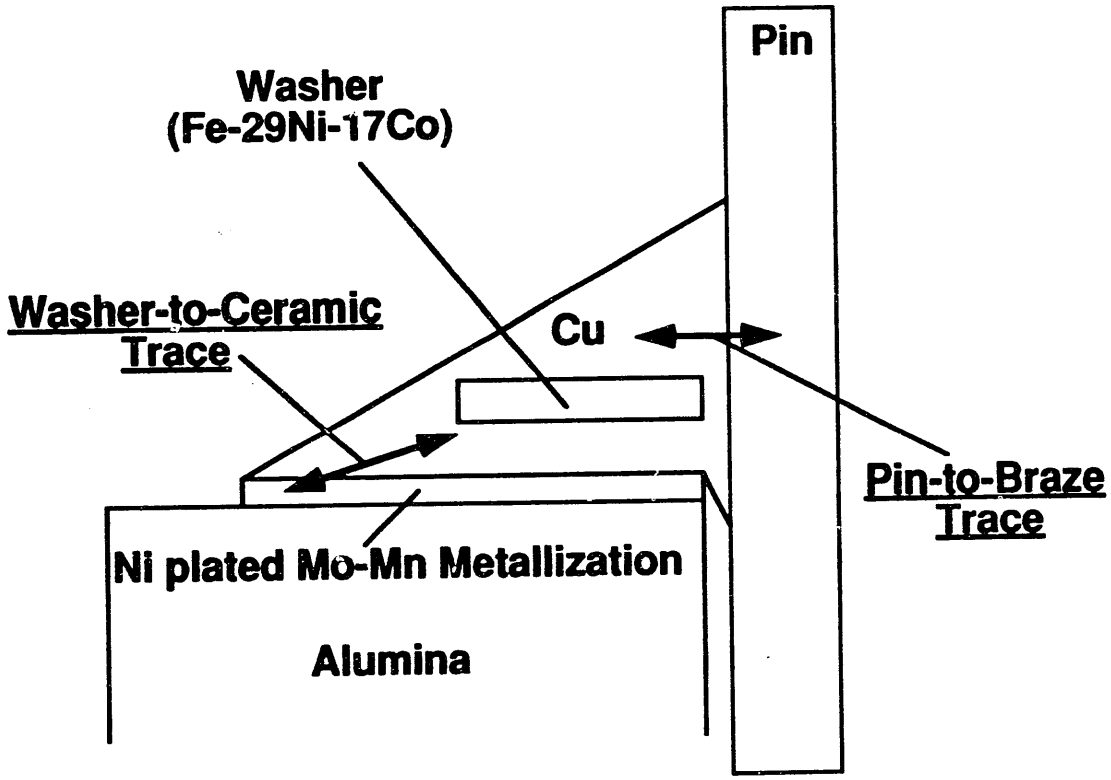

Figure 2 Schematic diagram showing the locations of the "Washer to Ceramic" and "Pin to Braze" electron microprobe linescans on the brazed area seal samples.

Figure 3 "Washer-to-Ceramic" electron microprobe linescan results for belt furnace brazed area seal samples containing a Palco™ alloy pin, using a relatively long thermal cycle. Both samples were processed using a braze cycle of 10 minutes above 1084°C with a peak temperature of 1109°C. (a) Single braze sample, with an average Cu content in this section of the braze equal to 89.57 wt.%. (b) Re-brazed sample, with an average Cu content in the braze equal to 86.96 wt.%.

Fig. 3a

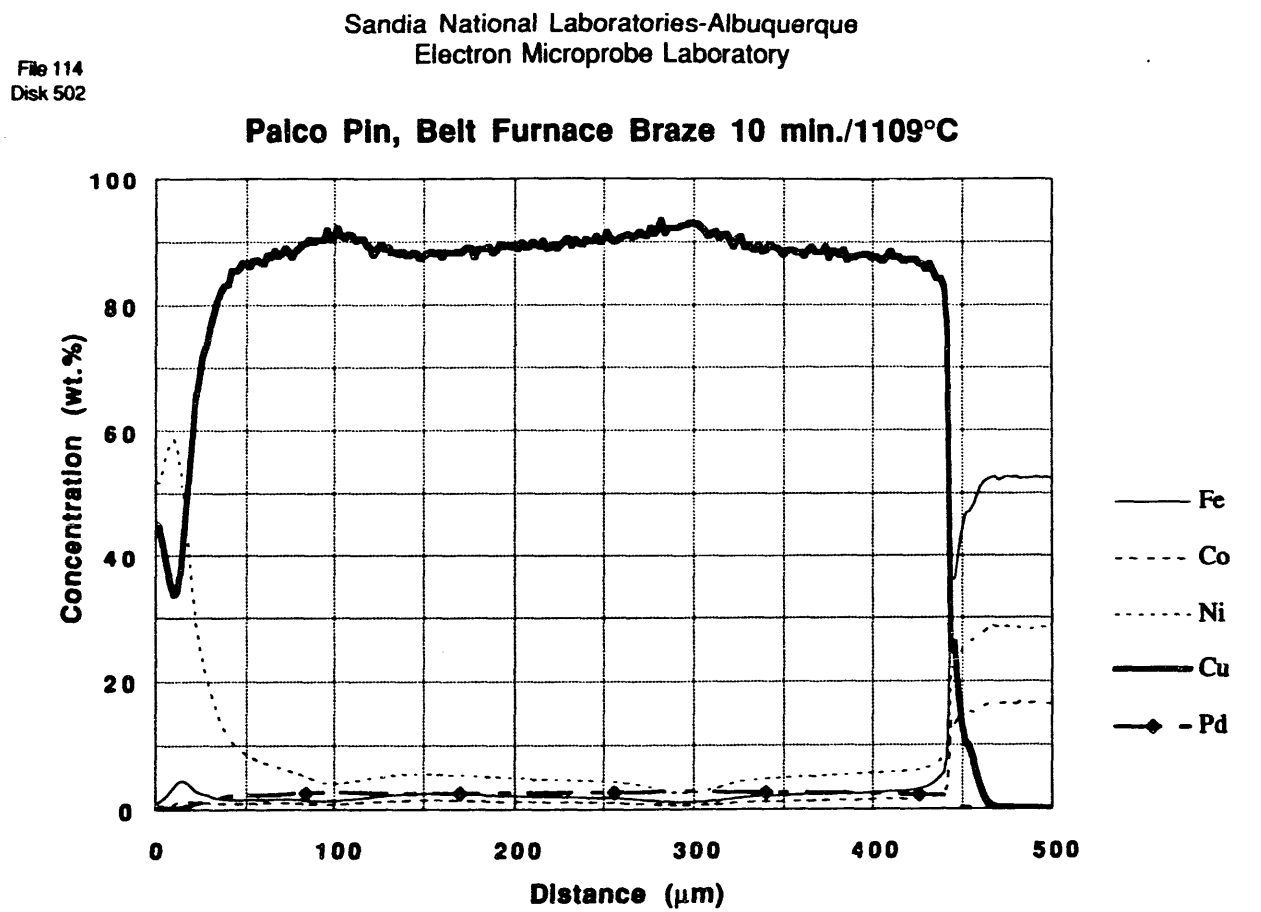

Fig 3a & b

Sandia National Laboratories-Albuquerque
Electron Microprobe Laboratory

File 104
Disk 502

Re-Brazed Belt Furnace with Palco Pin

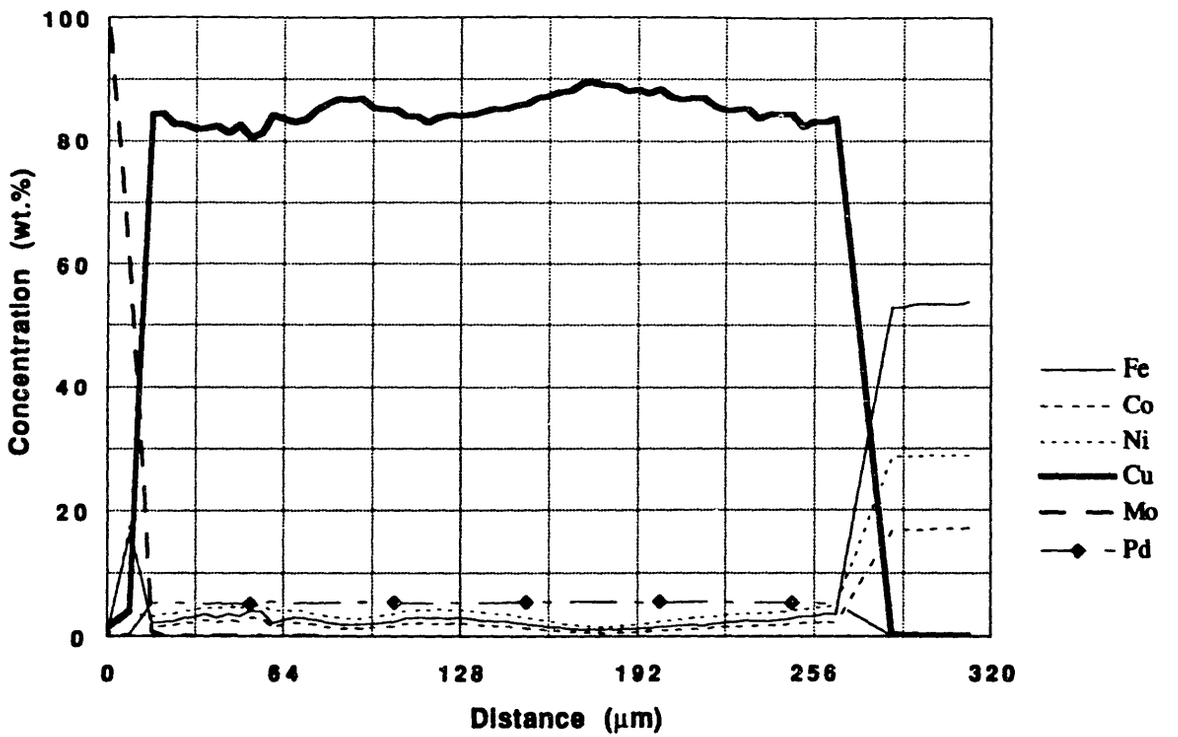

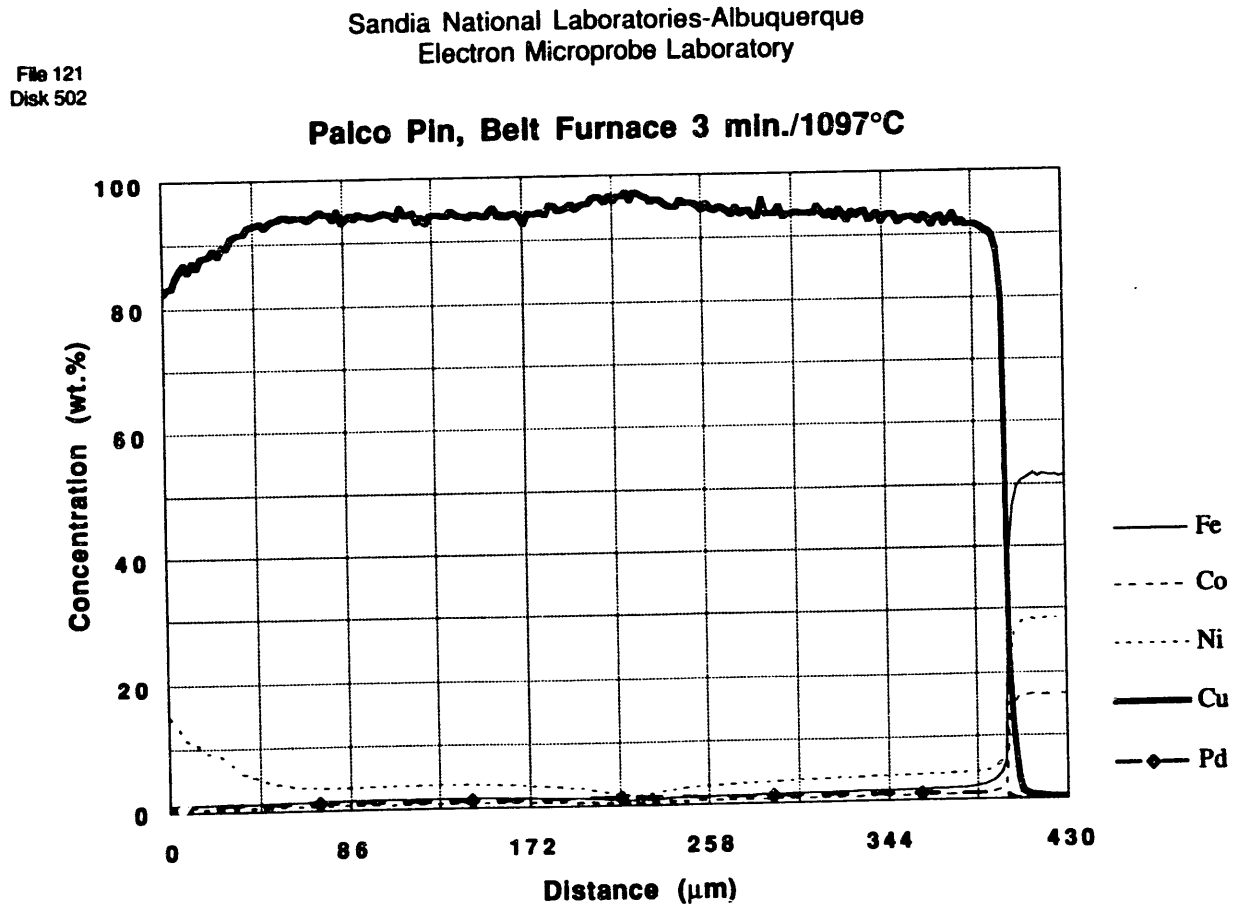

Figure 4 "Washer-to-Ceramic" electron microprobe linescan results for belt furnace brazed area seal samples containing a Palco™ alloy pin, using a relatively short thermal cycle. This sample was brazed using a thermal cycle of 3 minutes above 1084°C with a peak temperature of 1097°C. The average Cu content in this section of the brazement is 92.76 wt.%.

Fig 5a

Figure 5 "Washer-to-Ceramic" electron microprobe linescan results for batch furnace brazed area seal samples containing a Palco™ alloy pin, using the shortest possible thermal cycle. (a) Area seal brazed using a thermal cycle of 7 seconds above 1084°C with a peak temperature of 1087°C. The average Cu content in this section of the brazement is 99.68 wt.%. (b) Area seal brazed using a thermal cycle of 6 seconds above 1084°C with a peak temperature of 1090°C. The average Cu in this section of the brazement is 98.75 wt.%.

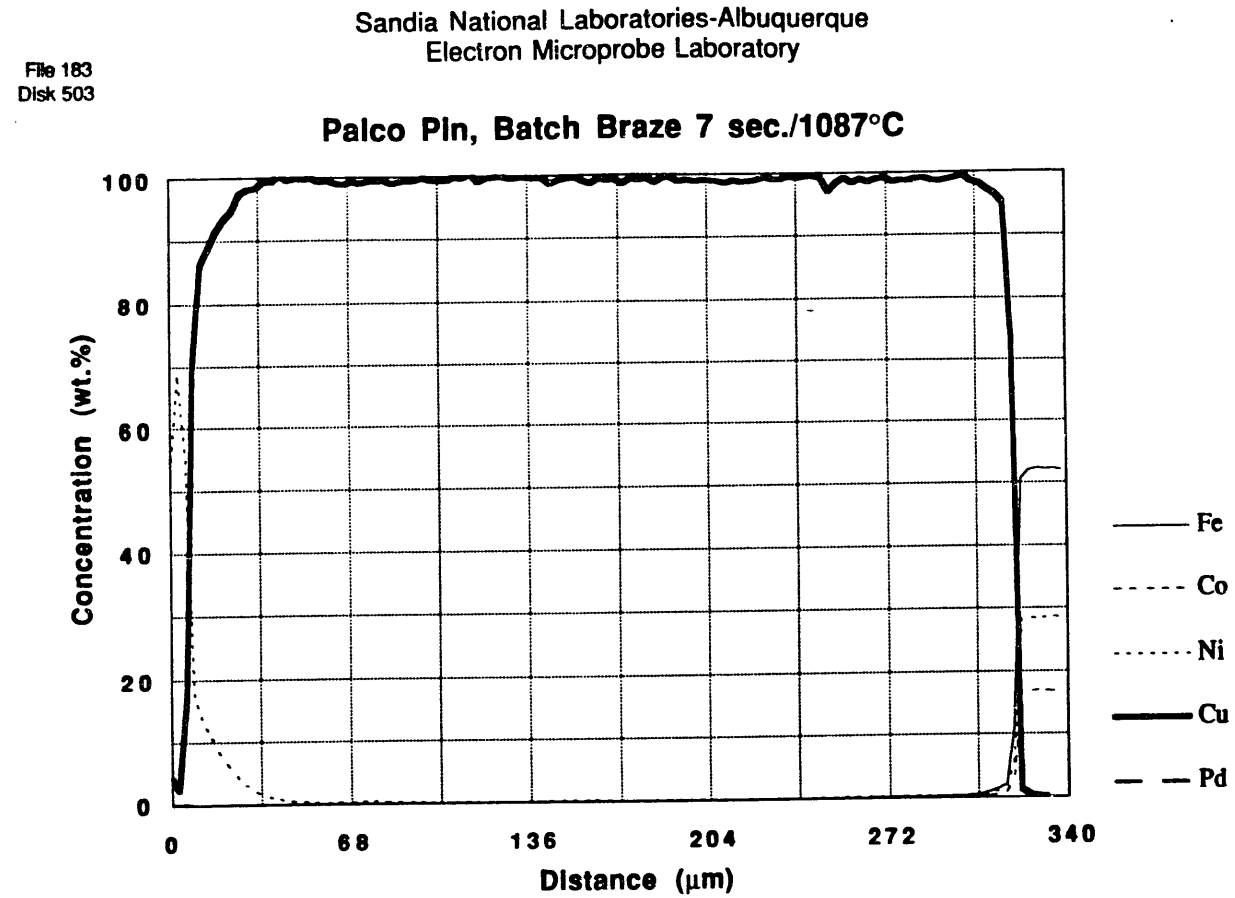

Fig 5b

Sandia National Laboratories-Albuquerque
Electron Microprobe Laboratory

File 185
Disk 503

Paico Pin, Batch Braze 6 sec./1090°C

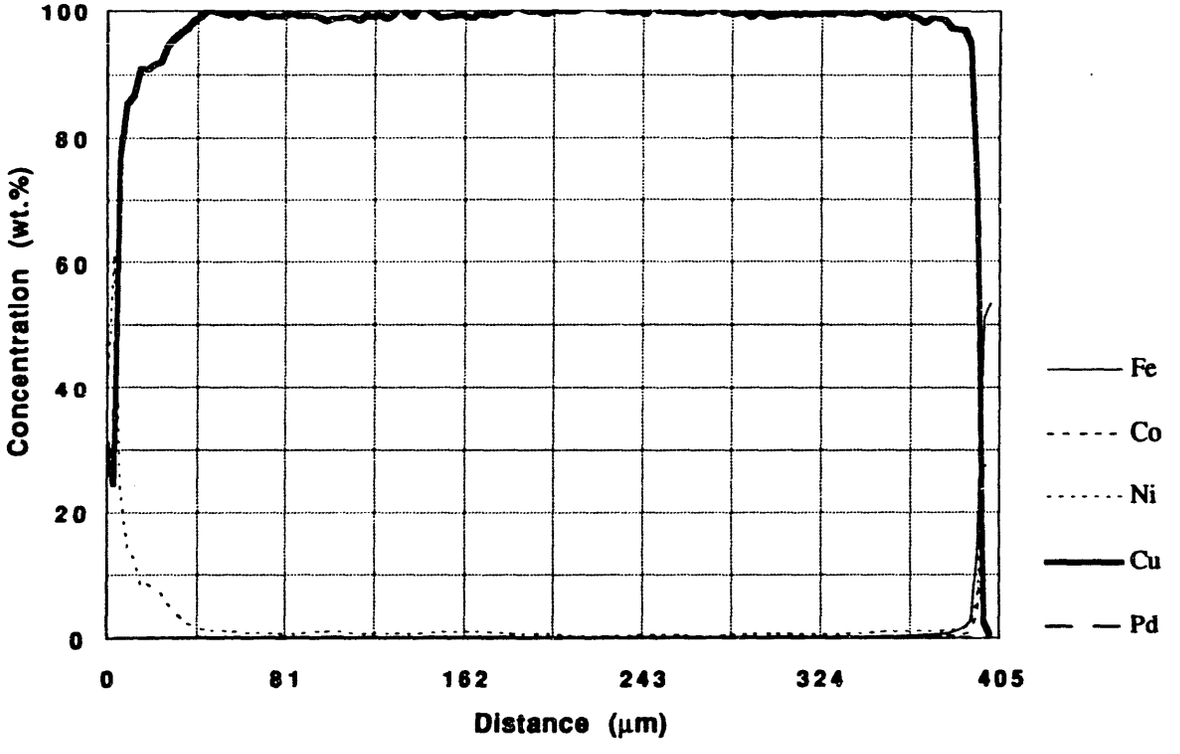

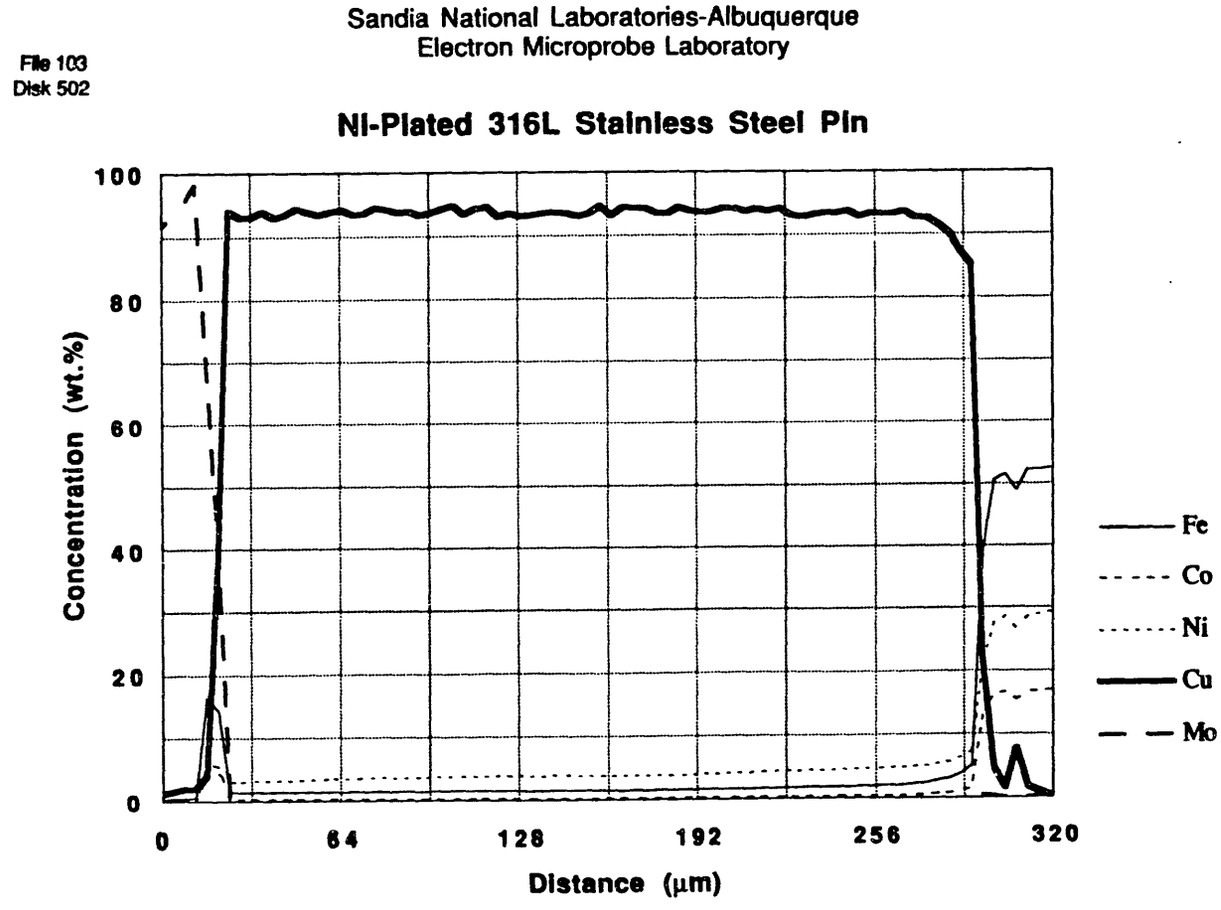

Figure 6 "Washer-to-Ceramic" electron microprobe linescan results for belt furnace brazed area seal samples containing a Ni-plated 316L stainless steel pin, with a braze thermal cycle of 10 minutes above 1084°C with a peak temperature of 1109°C.

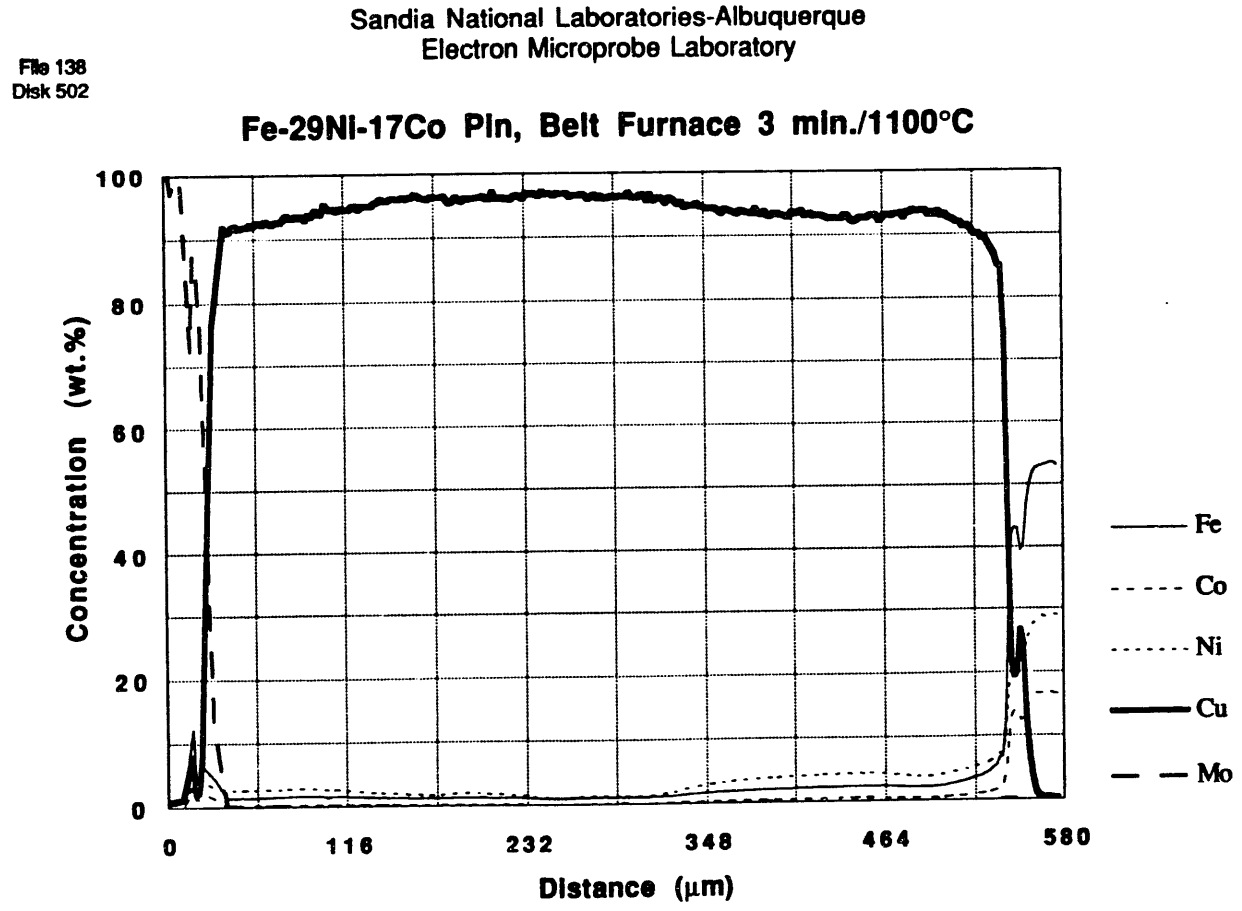

Figure 7 "Washer-to-Ceramic" electron microprobe linescan results for belt furnace brazed area seal samples containing a Fe-29Ni-17Co alloy pin, with a braze thermal cycle of 3 minutes above 1084°C with a peak temperature of 1100°C.

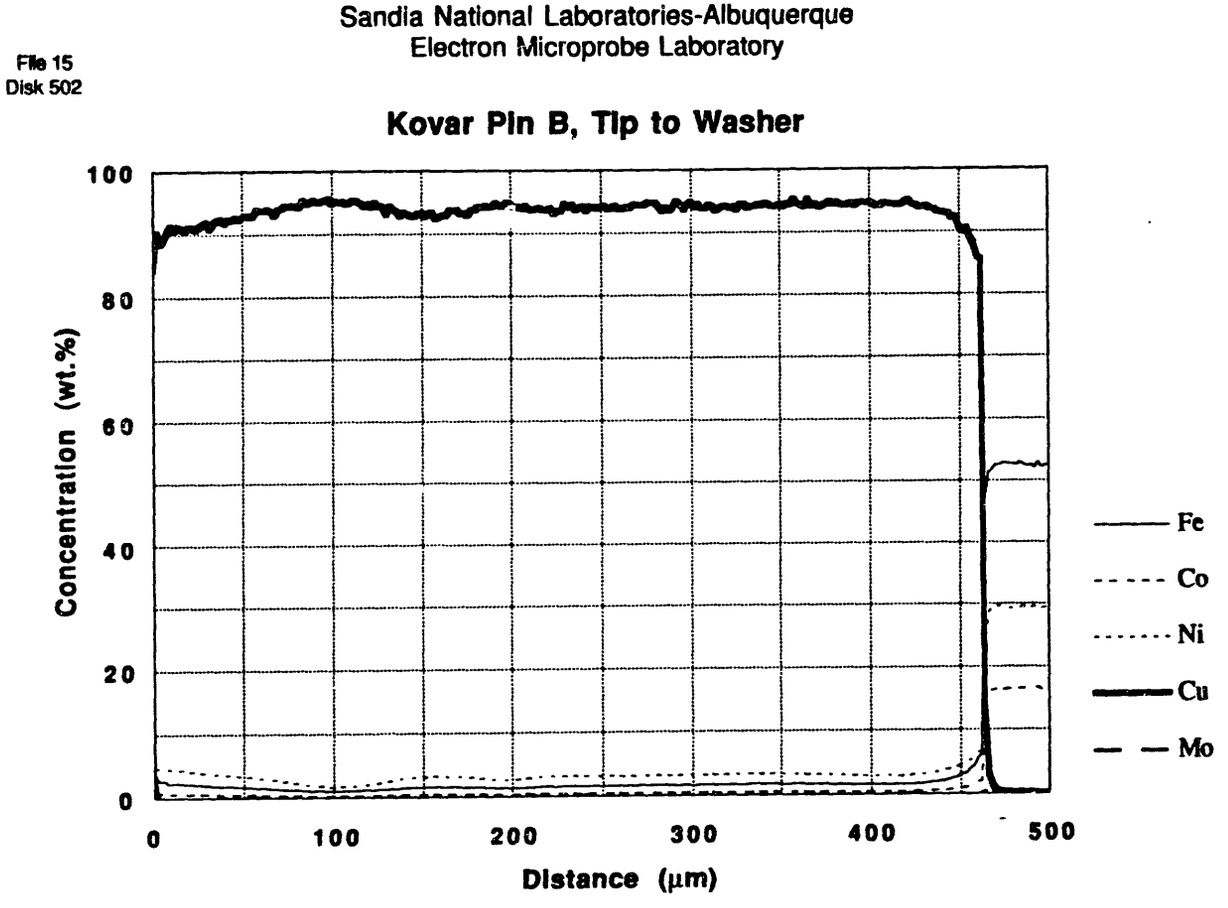

Figure 8 "Washer-to-Ceramic" electron microprobe linescan results for an area seal containing a Fe-29Ni-17Co alloy pin which was brazed for 10 minutes above 1084°C with a peak temperature of 1106°C. The average Cu content in this section of the brazement is 94.95 wt.%.

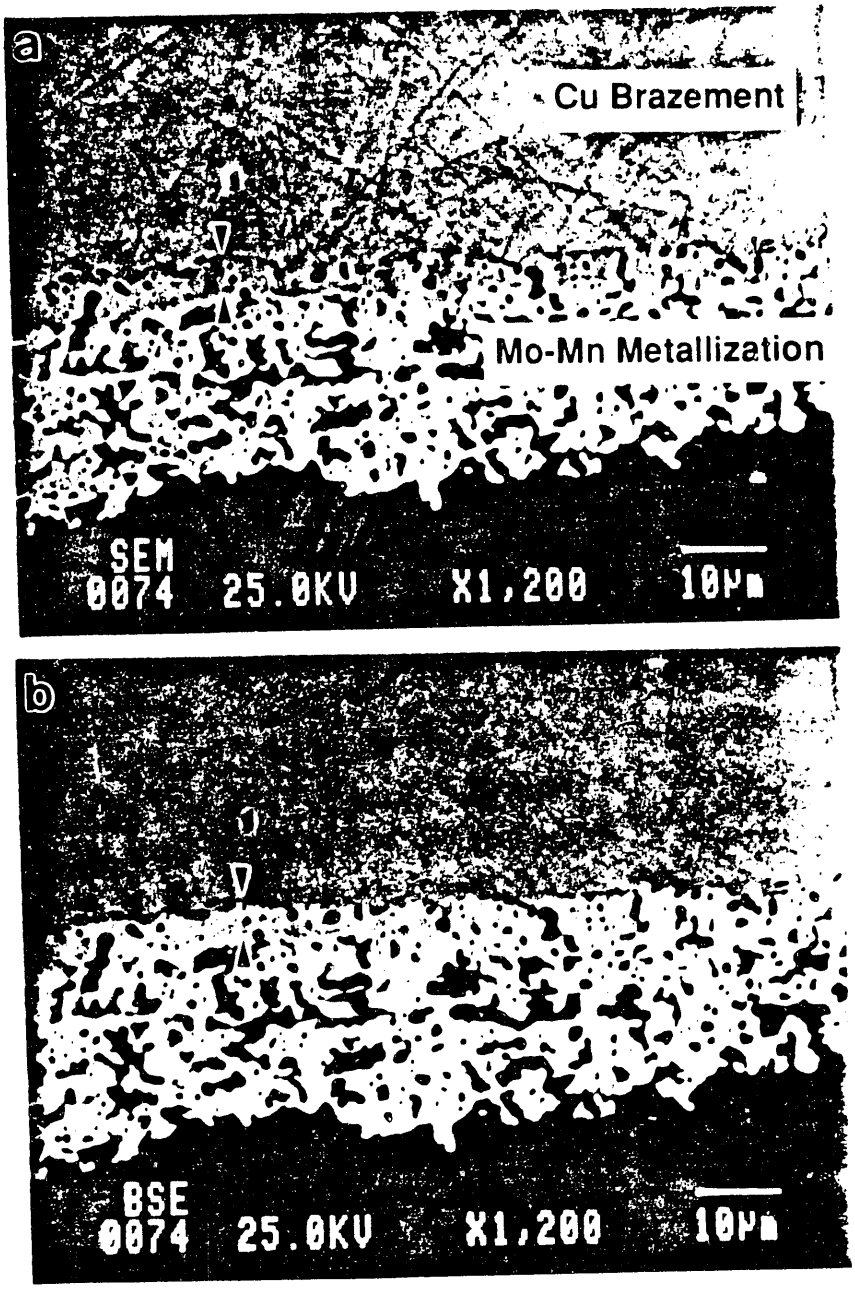

Figure 9 Scanning electron micrographs of the interfacial region showing the braze metal, Mo-Mn metallization and the alumina ceramic in a sample which was apparently re-brazed using the ten minute/1109°C cycle described in Figure 3. In both photos, the region between the arrows consists of the pseudobinary Mo-Fe-Co intermetallic compound roughly corresponding to $Mo_6(Fe_{3.5}Co_{3.5})_7$. (a) Secondary electron image. (b) Back-scattered electron image.

Fig. 10a.

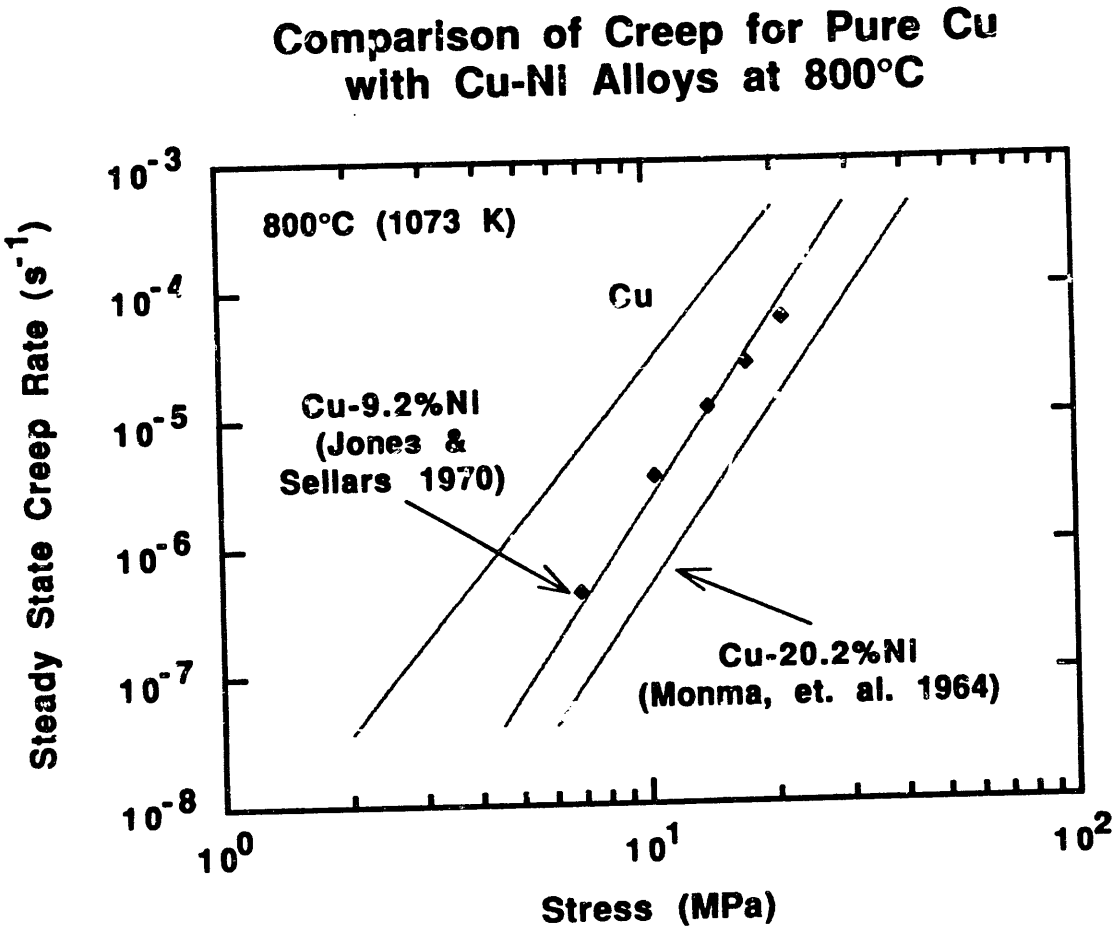

Figure 10 The effect of increasing Ni content on the steady-state creep rate of Cu alloys. Data on Cu-20.2 wt.% Ni are from Monma, et. al. (7), while the data for Cu-9.82 wt.% Ni are from Jones and Sellars (8). The correlations for pure Cu were developed in ref. 2. (a) Effect of alloying with Ni on the creep properties at 800°C. (b) Effect of alloying with Ni on the creep properties at 600°C.

Fig 10 b

Comparison of Creep for Pure Cu with Cu-Ni Alloys at 600°C

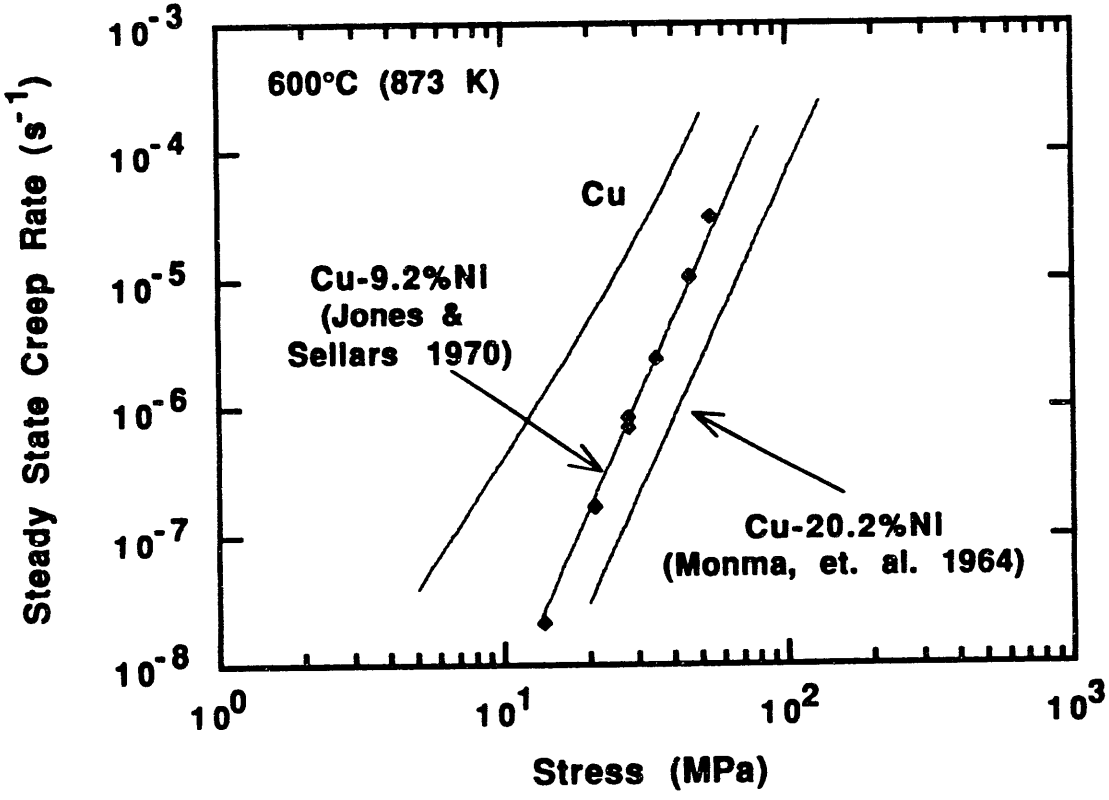

DATE
FILMED
10/13/93
END